Simulation of a 2D dam collapse problem using SPH method

Petr Jančík*[1]
[1] Department of Fluid Dynamics and Thermodynamics, Faculty of Mechanical Engineering, Czech Technical University in Prague, Technická 4, 166 07 Prague 6, Czech Republic

Abstract

In this paper, a numerical simulation of a dam break problem is presented. For this simulation, smoothed particle hydrodynamics (SPH) method was employed. SPH is a relatively non-conventional method, which can be used in CFD. Unlike traditional CFD methods, it uses a Lagrangian framework and it does not utilize computational mesh for a spatial discretization. Its Lagrangian nature allows to track particular fluid particles throughout a simulation easily; this tracking can help to describe some phenomena occurring in a problem. The dam break problem is described in detail and the simulation is compared with the experimental data which are available in the literature. In the end, the results are discussed and some improvements to the program to obtain better results are proposed.

Key-words: dam break; CFD; SPH; mesh-free; particle method

1. Introduction

A dam break is a relatively simple problem when in the beginning; initial and boundary conditions are easy to define. But when the liquid column begins to collapse situation is not so simple anymore. The free surfaces emerge and vanish throughout the process, and the flow is determined by inertia forces, which dominate over viscous and surface forces. It allows to use a simple inviscid fluid model and still get results which are not far from the reality if the free surface can be tracked appropriately. The mentioned features of the flow are the main reason why the dam break problem is used for testing of CFD programs which are intended to be used for free surface flow simulations. The problem is naturally three-dimensional but simulations are often simplified in two dimensions. It is much less computationally expensive and comparison with experimental data is still possible.

The dam break problem was used for validation of VOF (volume of fluid) method interface tracking algorithm for FVM (finite volume method) [1], SPH (smoothed particle hydrodynamics) [2], MPS (moving particle semi-implicit) [3, 4], and FEM (finite element method) [5]. The last three mentioned works combine both numerical and experimental investigation of the problem. The problem also served for comparison between various methods [6].

The fundamental experimental work on the dam break problem was published almost seventy years ago and it focused mainly on the kinematics of the flow [7]. Recently, an experimental work dealing with the dynamics of the flow was published [8]. These works provide data which are suitable for comparison with numerical results.

In this work, a dam break problem is investigated using SPH method. Unlike FVM, the most extensively used method in CFD, which uses the Eulerian reference frame, SPH is based on the Lagrangian description of the flow. Fluid is represented in the form of particles with constant mass and a mesh is not employed for spatial discretization. Therefore, it is referred to be one of the so-called mesh-free particle methods. The Lagrangian nature of the method was exploited to describe the phenomena occurring throughout the process.

*Corresponding author: Petr.Jancik@fs.cvut.cz

2. Method

The idea of the SPH method originates from an integral identity

$$a(\vec{x}) = \int_\Omega a(\vec{x'})\delta(\vec{x'} - \vec{x})\ \mathrm{d}V', \tag{1}$$

where a is an arbitrary function defined in a three-dimensional domain Ω and δ is the Dirac delta function. Vector $\vec{x}$ denotes coordinates of the specific point in Ω and $\vec{x'}$ is the variable of integration. This identity can be approximated in continuous form by replacing the Dirac delta function with smoothing function $W(\vec{x'} - \vec{x}, h)$, where h is smoothing length. It determines the size of the influence domain of the smoothing function. The next step is to substitute integration by summation over the particles, where infinitesimal volume $\mathrm{d}V'$ is replaced by particle volume expressed as m_j/ϱ_j. Thus the discrete approximation of the function is

$$a(\vec{x_i}) = \sum_j a(\vec{x_j}) W(\vec{x_j} - \vec{x_i}, h) \frac{m_j}{\varrho_j}. \tag{2}$$

Indices i and j serve for particle identification. Using relatively simple procedures, a discrete approximation of a function spatial derivative is obtained in the form

$$\nabla \cdot a(\vec{x_i}) = \sum_j a(\vec{x_j}) \cdot \nabla W(\vec{x_i} - \vec{x_j}, h) \frac{m_j}{\varrho_j}. \tag{3}$$

Note that the indices in the argument of the smoothing function W are swapped. This formulation allows transforming any partial differential equations into ordinary differential equations. For convenience, smoothing function gradient is usually written in the shortened form

$$\nabla W(\vec{x_i} - \vec{x_j}, h) = \nabla W_{ij}. \tag{4}$$

In this work, truncated Gaussian smoothing function was used. It is usually written in the form

$$W(R, h) = \begin{cases} \pi^{-\frac{d}{2}} h^{-d} e^{-R^2} & \text{if } R < 3 \\ 0 & \text{if } R \geq 3 \end{cases}, \tag{5}$$

where $R = |\vec{x}_j - \vec{x}_i|/h$ and d is number of spatial dimensions. Smoothing length h is set the same as the initial particle spacing.

2.1. Governing equations

The continuity and the momentum equations in the Lagrangian description are

$$\frac{\mathrm{D}\varrho}{\mathrm{Dt}} = -\varrho \nabla \cdot \vec{v}, \tag{6}$$

$$\frac{\mathrm{D}\tilde{\mathrm{v}}}{\mathrm{Dt}} = -\frac{1}{\varrho}\nabla p + \vec{f}. \tag{7}$$

The fluid is considered to be compressible and inviscid.

The system of equations needs to be closed by the equation of state. For weakly compressible SPH simulations, a popular choice is the Tait equation of state. It can be written in the form

$$p = \frac{c^2 \varrho_0}{\gamma}\left[\left(\frac{\rho}{\varrho_0}\right)^{\gamma} - 1\right] + p_0, \tag{8}$$

where ρ_0 is density at pressure p_0, c is speed of sound. Parameter $gamma = 7$ ensures that even small change in density leads to great variation in pressure. The Tait equation does not consider dependence on temperature. Since the changes in temperature are very small in the process, this non-physical assumption is justifiable. This barotropic fluid model also leads to the fact that the energetic equation is independent and it does not have to be solved. Instead of the physical speed of sound, it is taken a numerical value which should be set approximately ten times higher than expected maximal flow velocity in the solved problem [2]. That keeps variation in liquid density sufficiently low and the flow can be regarded as incompressible.

Using techniques which originate from the spatial derivative approximation (3) the governing equations (6) and (7) are obtained in the discrete form:

$$\frac{\mathrm{D}\varrho_{\mathrm{i}}}{\mathrm{Dt}} = \rho_i \sum_j \frac{m_j}{\varrho_j}(\vec{v}_i - \vec{v}_j)\cdot \nabla W_{ij} \tag{9}$$

$$\frac{\mathrm{D}\tilde{\mathrm{v}}_{\mathrm{i}}}{\vec{D}t} = -\sum_j m_j\Big(\frac{p_j}{\varrho_j^2} + \frac{p_i}{\varrho_i^2} + \Pi_{ij}\Big)\nabla W_{ij} + \vec{f}_i, \tag{10}$$

The symmetry with respect to the indices i and j reduces errors related to the particle discretization [9]. The term Π_{ij} is artificial viscosity and it serves for numerical stabilization [10]. Its value determined by the expression

$$\Pi_{ij} = \max\Big[-\frac{\alpha c_{ij} h_{ij}}{\varrho_{ij}}\frac{(\vec{v}_i - \vec{v}_j)\cdot \vec{x}_{ij}}{|\vec{x}_{ij}|^2 + \varepsilon h_{ij}^2}, 0\Big], \tag{11}$$

where α is tuning parameter and ε is singularity preventing coefficient. Variables c_{ij}, ϱ_{ij}, and h_{ij} denote mean values of the speed of sound, density, and smoothing length respectively. Vector $\vec{x}_{ij} = \vec{x}_i - \vec{x}_j$. The impact of the artificial viscosity should be sufficient to preserve numerical stability, but should not induce viscosity effects in the solution.

2.2. Boundary conditions

There are two types of boundaries in the dam break problem: free surface and wall. The free surface is tracked naturally by particle motion and no special treatment is needed. Wall modelling, on the other hand, is more complicated in particle methods than in mesh-based method. In this case, a very simple wall model was used. So-called virtual boundary particles are placed directly on the wall and generate repulsive force field acting on the fluid particles, which prevents them from penetrating the wall [2]. The force field is in the form of Lennard-Jones potential, thus

$$\vec{f}_i = D\Big[\Big(\frac{r_0}{|\vec{x}_{ij}|}\Big)^{p_1} - \Big(\frac{r_0}{|\vec{x}_{ij}|}\Big)^{p_2}\Big]\frac{\vec{x}_{ij}}{|\vec{x}_{ij}|^2}. \tag{12}$$

This formula applies only if $|\vec{x}_{ij}| \leq r_0$, otherwise $\vec{f} = \vec{0}$.

The advantage of the described way of enforcing boundary conditions is its simplicity. On the other hand, particles close to a boundary are not surrounded by neighbouring particles equally from all sides; they suffer from so-called particle deficiency. Consequently, pressure values evaluated near walls are incorrect.

2.3. Time integration

The discretized equations (9) and (10) are ordinary differential equations with the respect to time. To obtain the solution these equations have to be integrated. In this work, the modified leap-frog algorithm was employed for this purpose [9]. The algorithm can be written

$$\vec{v}_i{}^{\,n+\frac{1}{2}} = \vec{v}_i{}^{\,n-\frac{1}{2}} + \Delta t\Big(\frac{\mathrm{d}\vec{v}_i}{\mathrm{d}t}\Big)^n, \tag{13}$$

$$\rho_i^{n+\frac{1}{2}} = \rho_i^{n-\frac{1}{2}} + \Delta t\Big(\frac{\mathrm{d}\rho_i}{\mathrm{d}t}\Big)^n, \tag{14}$$

$$\vec{x}_i{}^{\,n+1} = \vec{x}_i{}^{\,n} + \Delta t\vec{v}_i{}^{\,n+\frac{1}{2}}, \tag{15}$$

$$\vec{v}_i{}^{\,n+1} = \vec{v}_i{}^{\,n+\frac{1}{2}} + \frac{\Delta t}{2}\Big(\frac{\mathrm{d}\vec{v}_i}{\mathrm{d}t}\Big)^n, \tag{16}$$

$$\rho_i^{n+1} = \rho_i^{n+\frac{1}{2}} + \frac{\Delta t}{2}\Big(\frac{\mathrm{d}\rho_i}{\mathrm{d}t}\Big)^n, \tag{17}$$

where indices in superscript denote time step. The leap-frog algorithm is an explicit integration method and therefore it is conditionally stable. To determine the size of the time step, it was used the Courant-Friedrichs-Lewy condition. Its form suitable for SPH stands

$$\Delta t \leq 0.25 \min_i \frac{h_i}{c_i}. \tag{18}$$

3. Numerical simulation

The dam break problem was simulated using the described method. The Lagrangian nature of the method enables to highlight some of the particles and it is possible to keep tracking them throughout the simulation. In this case, highlighted are the particles which reach above the original column height. This particle choice allows revealing some phenomena occurring in the flow.

3.1. Initial setup

The initial setup of the problem is in Fig. 1. The liquid column initial height $\eta_0 = 2$ m and initial width $\xi_0 = 1$ m. It is located adjacent to the left wall of the tank. The tank is 4 m wide and both its walls are 3 m tall.

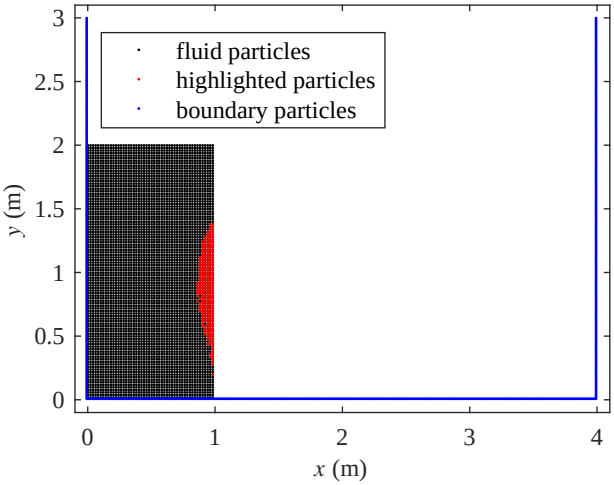

Fig. 1. *The dam break problem initial configuration.*

The liquid column is formed by 5000 particles of equal mass. Gravity is zero in the beginning of the simulation; the initial values of pressure and density of all the particles are p_0 and ϱ_0 respectively. Gravity is gradually switched on using the transition function

$$\zeta = 0.5\{\sin[(-0.5 + \frac{t}{t_{trans}})\pi] + 1\}, \qquad (19)$$

where t_{trans} is a transient time period [11]. During this period gravity gradually rises until it reaches its full magnitude. The transient time period is very small compared to the whole process, thus it does not affect the solution.

3.2. Results and discussion

The whole dam break problem process can be divided into three phases. In the initial phase, the surge front propagates until it hits the vertical wall. After that, the second phase begins. Its main feature is a presence of a rolling wave and its interactions. In the last phase, gravity waves move back and forth in the tank and liquid motion is gradually damped.

3.2.1. Surge front propagation phase

In the initial phase of the dam break, the liquid column collapsed and the surge front headed towards the right wall (Fig. 2 and Fig. 3). In both these figures, a group of disrupted particles adjacent to the left wall is clearly visible. Also, the group of highlighted particles got closer to the surge front compared to the initial setup. The explanation for these phenomena is the fact that the utilized wall boundary condition is not a true free-slip boundary condition. The repulsive force generated by the boundary particles is not exactly normal to the boundary, but it also has a tangent component.

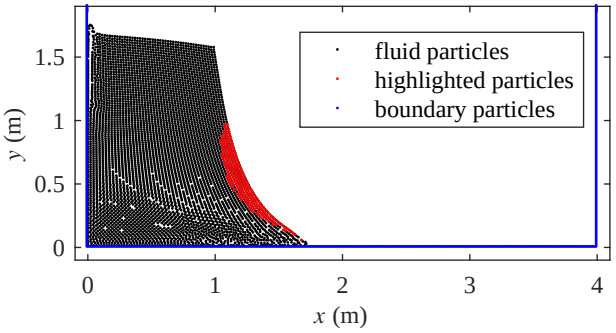

Fig. 2. *The initial phase of the dam break; the surge front moved towards the right wall. Time* $t = 0.3$ s.

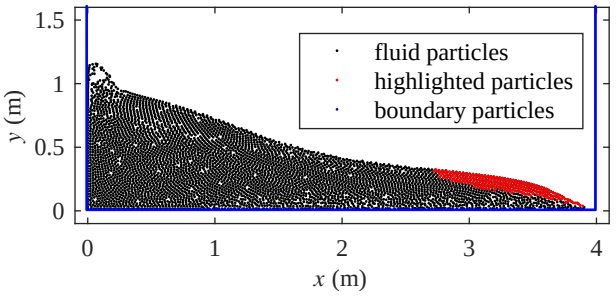

Fig. 3. *The initial phase of the dam break; just before the surge front hit the right wall. Time* $t = 0.7$ s.

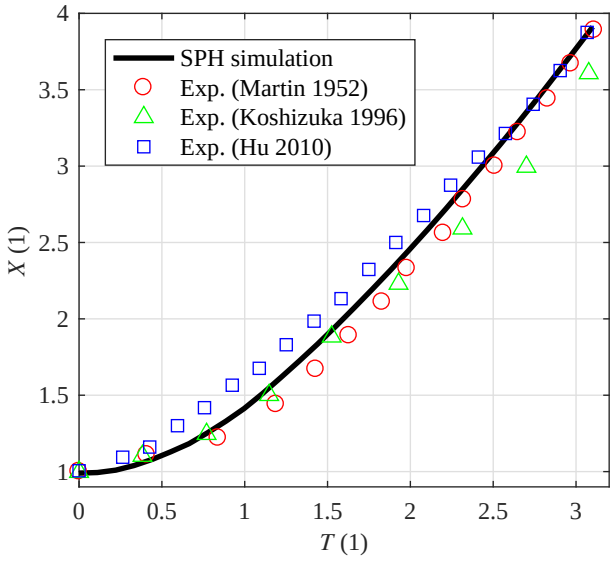

Fig. 4. *Dimensionless surge front position as a function of dimensionless time; simulation and experiment comparison. Martin 1952 [7], Koshiuzuka 1996 [3], Hu 2010 [4].*

The surge front position during the initial phase was compared with experimental data previously published by some other authors (Fig. 4). The comparison has to be performed in dimensionless variables since the experiments and the numerical simulation were different in their size. Only the column height to width ratio is kept the same (2:1). The dimensionless surge front position and time are defined as

$$X = \frac{\xi}{\xi_0}, \quad T = t\sqrt{\frac{2g}{\xi_0}} \qquad (20)$$

where ξ is the surge front position and ξ_0 is the initial liquid column width.

Discrepancies between the experimental data can be explained by the different experimental devices, and measuring methods. The simulation and the experiments seem to be in a good agreement. The imperfect free-slip boundary condition described previously seems to have a little effect on the fluid motion globally. The surge front reached the velocity corresponding to the free fall velocity from the height of the original liquid column ($|\vec{v}| = \sqrt{2|\vec{g}|\eta_0}$).

3.2.2. Rolling wave phase

The rest of the simulation was compared with experimental and numerical data from a qualitative point of view only. The same phenomena are to be found in both experimental and numerical investigation in [3] as in herein presented simulation. Particular data for comparison were chosen with regard to similarity of both cases.

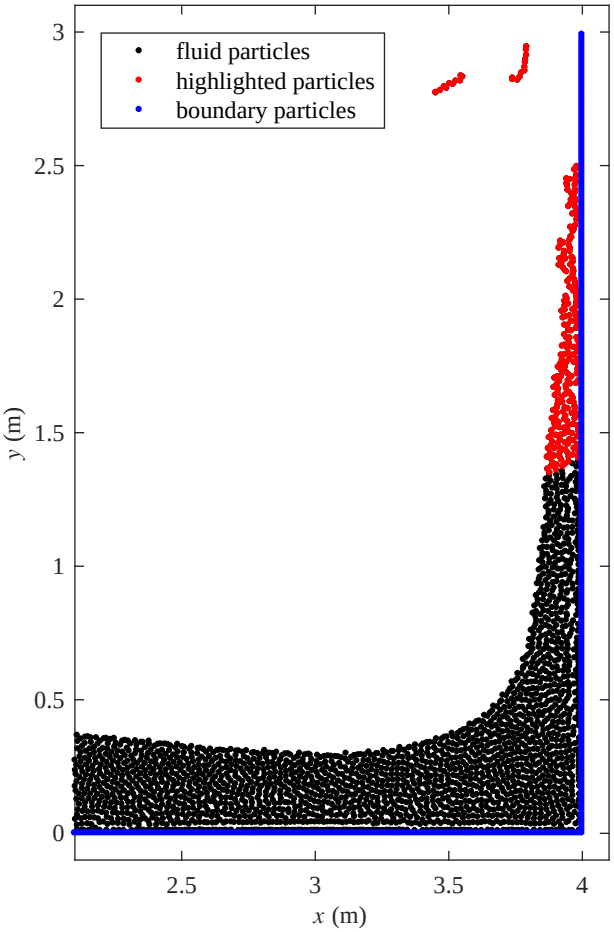

Fig. 5. *Detail of the vertical jet formed along the right wall after the surge front impacted the wall. Time* $t = 1.1$ s.

As the surge front reached the right wall, the fluid decelerated rapidly. That led to a significant rise in pressure in the bottom right corner. This high-pressure domain affected the surrounding fluid which was accelerated again; in the vertical direction mostly. Consequently, a vertical jet was formed along the right wall (Fig 5). The top of the jet reaches the height about one and half times greater than the original column height. Some particles even separate from the main liquid body and reach the height of more than twice the original column height

Then the top of the jet started losing its momentum, while the bottom part was still moving upwards. This led to a creation of the rolling wave (Fig. 6). It moved back towards the left wall, and its tip hit the liquid surface. The impacting liquid then rebounded from the surface, creating another liquid jet (Fig. 7). This process created closed pockets of void space. However, all these empty pockets vanished in a short time.

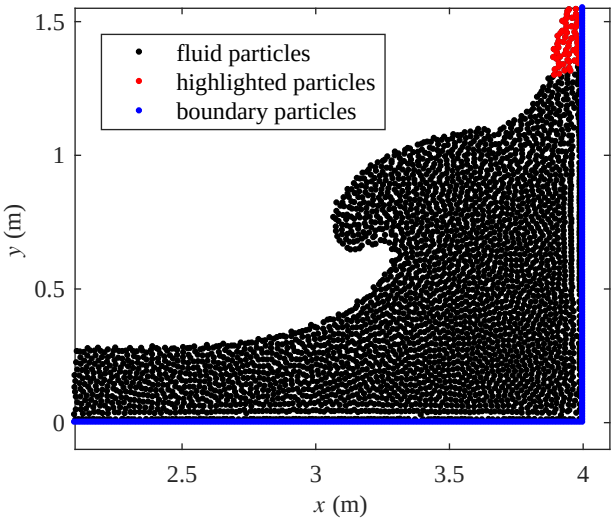

Fig. 6. *Detail of the rolling wave before the impact on the surface. Time* $t = 1.85$ s.

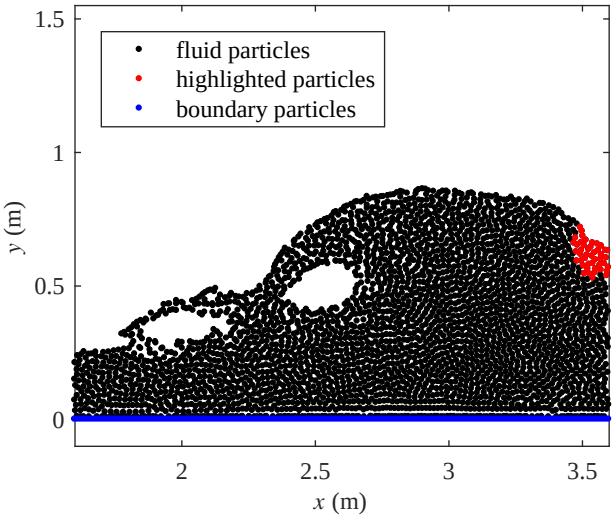

Fig. 7. *Detail of the rolling wave after the impact on the surface. Void pockets are clearly visible. Time* $t = 2.15$ s.

3.2.3. Gravity wave phase

When the wave impacted the left wall, a vertical jet along the wall emerged again, but this time having significantly less momentum (Fig. 8). This amount of momentum was not enough to create a rolling wave. Instead of that, a surface gravity wave emerged (Fig. 9). This wave reflected from the walls and the fluid motion was gradually damped.

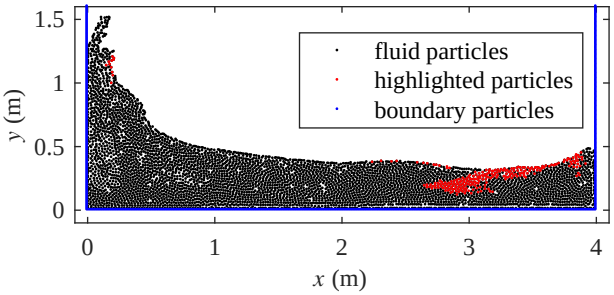

Fig. 8. *The impact on the left wall. Created jet is much smaller then previously. Time* $t = 3.3$ s.

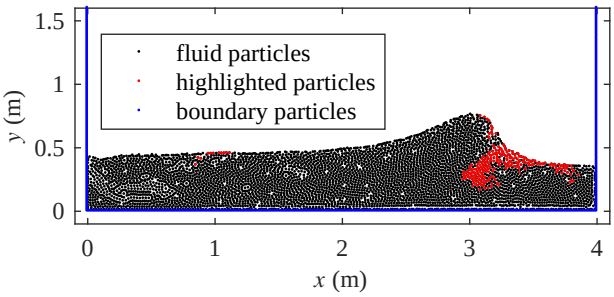

Fig. 9. *The surface gravity wave moving towards the right wall. Time* $t = 4.5$ s.

4. Conclusion and future work

In this work, a dam break problem was solved using SPH method, which is a mesh-free particle method. The method itself is briefly introduced and some used algorithms are described in detail. The initial phase of the problem was compared with experimental data available in the literature. The numerical results are in a good quantitative agreement with these data. The later phases of the simulation were also compared with the experiments and numerical results of other authors. Only the qualitative comparison could be done and the agreement is good again. The phenomena occurring throughout the simulation are described in detail. For this purpose, the Lagrangian nature of the method was exploited; certain particles were tracked throughout the simulation.

The current implementation of the SPH method proved itself to be capable of free surface flow simulations. Free surfaces are tracked naturally by the particle motion. The solution overall is in good agreement with the numerical and experimental data of other authors, despite a very simple method of enforcing wall boundary condition. To further improve the results, a more sophisticated method should be implemented. Relatively simple and robust methods are, e.g. [11, 12]. Both these methods deal with a particle deficiency, which is crucial for evaluation of variables close to a wall. The employed weakly compressible approach of modelling incompressible flow also leads to strong oscillations in the pressure field. Kinematics of the flow seems not to be affected by these oscillations. To reduce them, a diffusive term can be introduced into continuity equation [13].

Acknowledgement

This work was supported by the Grant Agency of the Czech Technical University in Prague, grant No. SGS18/124/OHK2/2T/12.

Nomenclature

Subscript indices i and j denote particles, index 0 labels reference value. Superscript index denotes time step.

a	arbitrary function	(1)
c	speed of sound	$(\mathrm{m}\cdot\mathrm{s}^{-1})$
D	boundary repulsive force coefficient	$(\mathrm{m}^2\cdot\mathrm{s}^{-2})$
d	number of spatial dimensions	(1)
$\mathrm{d}V'$	infinitesimal volume	(m^3)
$\vec{f}$	external force field vector	$(\mathrm{m}\cdot\mathrm{s}^{-2})$
$\vec{g}$	gravity force field vector	$(\mathrm{m}\cdot\mathrm{s}^{-2})$
h	smoothing length	(m)
m	mass	(kg)
p	pressure	(Pa)
R	dimensionless distance	(1)
T	dimensionless time	(1)
t	time	(s)
$\vec{v}$	velocity vector	$(\mathrm{m}\cdot\mathrm{s}^{-1})$
W	smoothing function	$(\mathrm{m}^{-\mathrm{d}})$
X	dimensionless surge front position	(1)
$\vec{x}$	position vector	(m)
α	artificial viscosity coefficient	(1)
γ	equation of state exponent	(1)
Δt	time step	(s)
δ	Dirac delta function	$(\mathrm{m}^{-\mathrm{d}})$
ε	singularity preventing coefficient	(1)
ζ	transition function	(1)
ξ	surge front position	(m)
Π	artificial viscosity term	$(\mathrm{kg}^{-1}\cdot\mathrm{m}^5\cdot\mathrm{s}^{-2})$
ϱ	density	$(\mathrm{kg}\cdot\mathrm{m}^{-3})$
η	column height	(m)
Ω	domain in d-dimensional space	$(\mathrm{m}^{\mathrm{d}})$

References

[1] C. W. Hirt and B. D. Nichols. "Volume of fluid (VOF) method for the dynamics of free boundaries". In: *Journal of Computational Physics* 39.1 (1981), pp. 201–225. ISSN: 0021-9991. DOI: 10.1016/0021-9991(81)90145-5.

[2] J. J. Monaghan. "Simulating free surface flows with SPH". In: *Journal of Computational Physics* 110.2 (1994), pp. 399–406. ISSN: 0021-9991. DOI: https://doi.org/10.1006/jcph.1994.1034.

[3] S. Koshizuka and Y. Oka. "Moving-particle semi-implicit method for fragmentation of incompressible fluid". In: *Nuclear Science and Engineering* 123.3 (1996), pp. 421–434. DOI: 10.13182/NSE96-A24205.

[4] C. Hu and M. Sueyoshi. "Numerical simulation and experiment on dam break problem". In: *Journal of Marine Science and Application* 9.2 (2010), pp. 109–114. ISSN: 1993-5048. DOI: 10.1007/s11804-010-9075-z.

[5] M. A. Cruchaga, D. J. Celentano, and T. E. Tezduyar. "Collapse of a liquid column: Numerical simulation and experimental validation". In: *Computational Mechanics* 39.4 (2007), pp. 453–476. ISSN: 1432-0924. DOI: 10.1007/s00466-006-0043-z.

[6] G. Colicchio et al. "Free-surface flow after a dam break: A comparative study". In: *Ship Technol. Res.* 49.3 (2002), pp. 95–104.

[7] J. C. Martin et al. "Part IV. An experimental study of the collapse of liquid columns on a rigid horizontal plane". In: *Philosophical Transactions of the Royal Society of London A: Mathematical, Physical and Engineering Sciences* 244.882 (1952), pp. 312–324. ISSN: 0080-4614. DOI: 10.1098/rsta.1952.0006.

[8] L. Lobovský et al. "Experimental investigation of dynamic pressure loads during dam break". In: *Journal of Fluids and Structures* 48 (2014), pp. 407–434. ISSN: 0889-9746. DOI: 10.1016/j.jfluidstructs.2014.03.009.

[9] G. R. Liu and M. B. Liu. *Smoothed particle hydrodynamics - A meshfree particle method*. World Scientific, 2003. ISBN: 9789812564405.

[10] J. J. Monaghan. "Smoothed particle hydrodynamics". In: *Annual Review of Astronomy and Astrophysics* 30.1 (1992), pp. 543–574. DOI: 10.1146/annurev.aa.30.090192.002551.

[11] S. Adami, X. Hu, and N. Adams. "A generalized wall boundary condition for smoothed particle hydrodynamics". In: *Journal of Computational Physics* 231 (2012), 7057–7075. DOI: 10.1016/j.jcp.2012.05.005.

[12] M. B. Liu, J. R. Shao, and J. Z. Chang. "On the treatment of solid boundary in smoothed particle hydrodynamics". In: *Science China Technological Sciences* 55.1 (2012), pp. 244–254. ISSN: 1869-1900. DOI: 10.1007/s11431-011-4663-y.

[13] D. Molteni and A. Colagrossi. "A simple procedure to improve the pressure evaluation in hydrodynamic context using the SPH." In: *Computer Physics Communications* 180.6 (2009), pp. 861–872. DOI: 10.1016/j.cpc.2008.12.004.